ISSN 1070-3284, Russian Journal of Coordination Chemistry, 2020, Vol. 46, No. 4, pp. 224–240. © Pleiades Publishing, Ltd., 2020.
Russian Text © The Author(s), 2020, published in Koordinatsionnaya Khimiya, 2020, Vol. 46, No. 4, pp. 204–220.

Homoligand Tris-*o*-Dioxolene Complexes. Peculiarities of the Molecular Structures and Magnetic Properties

M. P. Bubnov[a], *, A. V. Piskunov[a], A. A. Zolotukhin[a], I. N. Meshcheryakova[a], N. A. Skorodumova[a], A. S. Bogomyakov[b], E. V. Baranov[a], G. K. Fukin[a], and V. K. Cherkasov[a]

[a] *Razuvaev Institute of Organometallic Chemistry, Russian Academy of Sciences, Nizhny Novgorod, Russia*
[b] *International Tomography Center, Siberian Branch, Russian Academy of Sciences, Novosibirsk, Russia*
**e-mail: bmp@iomc.ras.ru*

Received October 4, 2019; revised October 22, 2019; accepted October 31, 2019

Abstract—Metal tris-*o*-dioxolene (*o*-quinone, *o*-semiquinone, and catecholate) complexes represent an interesting and vivid model system for the demonstration of a relationship between the structure and magnetic properties when considering a series of objects of the same type. After publishing the reviews [1, 2], the metal tris-*o*-dioxolene complexes containing the symmetric 3,6-di-*tert*-butyl-*o*-benzoquinone derivatives with substituents in positions 4 and 5 are described in a number of works. In addition, some earlier unpublished structures of the complexes of this type are reviewed. The substituents in the lateral chains enhance the steric protection of the metal center and, as a consequence, result in the formation of coordination polyhedra uncharacteristic of the tris(dioxolene) complexes, such as a trigonal prism. In turn, the distortion of the structure affects the magnetic properties of the complexes. Only the complexes with the derivatives of sterically hindered *o*-quinones, 3,5- and 3,6-di-*tert*-butyl-*o*-benzoquinones, are considered in the present review. On the one hand, bulky *tert*-butyl groups prevent the formation of direct intermolecular contacts and, on the other hand, prevent organic reactions to occur at the benzoquinone cycle.

Keywords: free-radical complexes, *o*-quinones, *o*-semiquinones, catecholates, magnetic interactions, molecular structure

DOI: 10.1134/S107032842003001X

INTRODUCTION

A combination of a transition metal with redox-active ligands, among which is *o*-dioxolene, induces ambiguous interpretations of the charge distribution between them. The ratio of their redox potentials occupies the first place among the factors determining the valent and spin states of both the metal and ligand. However, the steric hindrance of *o*-dioxolene should be taken into account, since this factor (together with the ionic radius of the metal) determines, on the one hand, the geometry of the coordination mode and, on the other hand, can directly affect the metal–ligand distance. The redox transformations of substituted *o*-quinone are presented in Scheme 1.

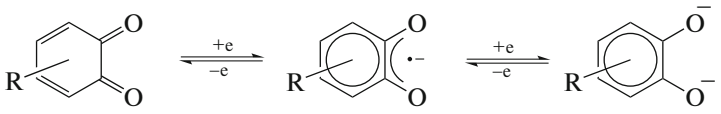

Scheme 1.

A series of cobalt compounds with di-*tert*-butyl-*o*-benzoquinones can serve as an example of the influence of the steric hindrance of *o*-dioxolenes on the properties of the homoligand complexes formed by these dioxolenes. Owing to the oxygen atom unprotected by the *tert*-butyl group, nonsymmetric 3,5-di-*tert*-butyl-*o*-benzoquinone (3,5-DBQ) forms the tetrameric complex $[Co(3,5\text{-}DBSQ)_2]_4$ (3,5-DBSQ is the radical anion of 3,5-DBQ) in which cobalt exists in the divalent high-spin state [3]. Symmetric 3,6-di-*tert*-butyl-*o*-benzoquinone (3,6-DBQ) forms a pseudooctahedral polyhedron with trivalent low-spin cobalt [4]. The presence of the piperazine bicycle in positions 4 and 5 of 3,6-DBQ annelated via the *N*,*N*' nitrogen atoms (3,6-DBQ-pipe) results in the structure of an ideal trigonal prism. The magnetic properties of this complex cannot be interpreted unambiguously [5]. Sterically

hindered *o*-quinones described in this review are presented in Scheme 2 (3,6-DBQ-gly is 3,6-di-*tert*-butyl-*o*-benzosemiquinone with the *O*,*O*'-ethylenediolate cyclic substituent in positions 4 and 5 (hereinafter, Q, SQ, and Cat are neutral *o*-quinone, its radical anion, and its dianion, respectively).

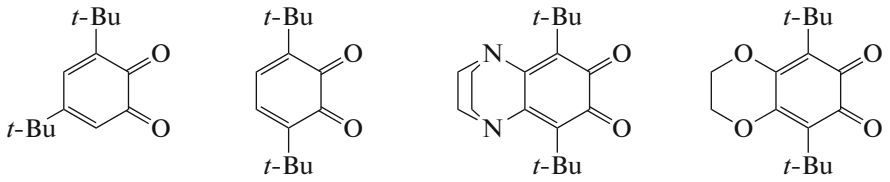

3,5-DBQ 3,6-DBQ 3,6-DBQ-pipe 3,6-DBQ-gly

Scheme 2.

Various metals, being in the same-type environment of three dioxolene ligands, exist in different valent and spin states, which in combination with a variety of structural polyhedra leads to a wide range of magnetic properties of the tris(dioxolene) complexes. The exchange interaction vary from the strongly antiferromagnetic interaction for chromium tris(semiquinolates) [6] to weak ferromagnetic one for the aluminum and gallium complexes [4].

The complexes of the general type M(dioxolene)$_3$ synthesized in the last century were described in detail [1]. The author of this review examined bond lengths in many *o*-quinone complexes of transition metals and concluded that the redox state of the dioxolene ligand can be determined from the bond lengths in the coordination five-membered cycle –O–C–C–O–M– ignoring the ionic radius of the metal [7]. The validity of these observations was proved later by the calculations [8]. The task of the present work is to describe the new complexes in the framework of the general regularities found earlier [1], first of all, their structural peculiarities and related magnetic properties. In addition, a restricted range of the complexes is reviewed [1]: the compounds with sterically hindered *o*-quinones. The rest part of the complexes is presented by *o*-chloranil and 9,10-phenanthrenequinone for which the structural features are determined, to a high extent, by the packing and the magnetic properties are determined by the intermolecular magnetic exchange.

RESULTS AND DISCUSSION

The description of the properties of the complexes on the basis of the distribution over groups to which metal-complexing agents belong in the periodic system of elements seems to be most reasonable. Cadmium is the only metal of Group II for which the M(dioxolene)$_3$ complex was structurally characterized. The similar magnesium compound [9] was not structurally characterized. Compound (3,6-DBQ)Cd(3,6-DBSQ)$_2$ (**1**) was synthesized by the reaction of cadmium amalgam with the corresponding *o*-quinone [10] and was studied by X-ray structure analysis. Each of two crystallographically independent molecules of the complex contains two ligands with the bond length distribution typical for the semiquinone coordination mode, and one ligand has pronounced C=O and C=C double bonds belonging to coordinated *o*-quinone. The geometry of the internal coordination sphere in both molecules is distorted to such an extent that can hardly be assigned to any type of coordination environment. Here an idea of "twist angle" should be introduced for the further discussion of coordination polyhedra: the value that quantitatively characterizes intermediate forms of hexacoordinated tris(chelate) complexes between an octahedron and a trigonal prism [11]. Octahedra and trigonal prisms are characterized by the 3-fold symmetry axis. The projection along this axis in the octahedron looks like two isosceles triangles turned by 60° and imposed on each other (Fig. 1). The same projection in the trigonal prism looks like a triangle. Thus, the twist angle α for the octahedron is 60°, while that for the trigonal prism is 0°. In the case of the tris(dioxolene) complexes, the twist angle was determined separately for each ligand as follows: a centroid is constructed in the projection along the 3-fold axis on the basis of three oxygen atoms and forms the lower triangle, and a centroid forming the upper triangle is constructed. The torsion angle for a given ligand is determined by four points: centroid 1–O(1)–O(2)–centroid 2.

The twist angle in complex **1** is 34.09°–38.03°. The OMO angles for the oxygen atoms occupied the *trans* position to each other are 102.47°, 140.42°, and 161.13° for one molecule and 145.05°, 152.70°, and 170.96° for another molecule. This angle is 180° for the octahedron and 133° for the trigonal prism. A distinction feature of the geometry of neutral *o*-quinone is a break along the O...O line, the angle of which is 28.64° for one molecule and 25.55° for the second molecule. These are much higher than the values for semiquinones: 9.12° and 18.38° for one molecule and 8.25° and 15.57° for the second molecule.

The magnetic behavior of the complex is determined by its composition: two unpaired electrons on two semiquinones nearly do not interact (Fig. 2). The

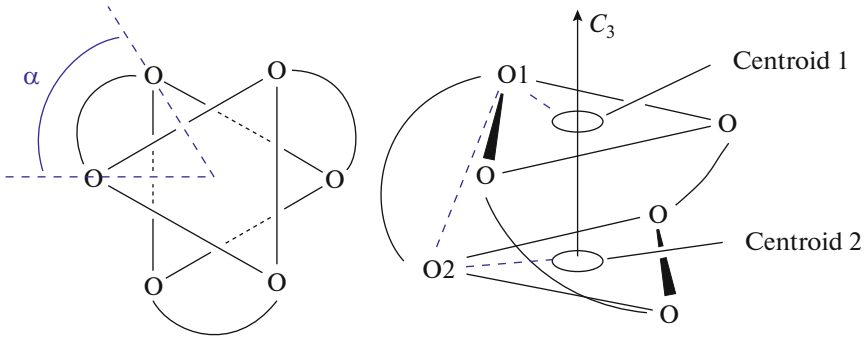

Fig. 1. Illustration of an idea of "twist angle." The torsion angle is shown by the blue dashed line.

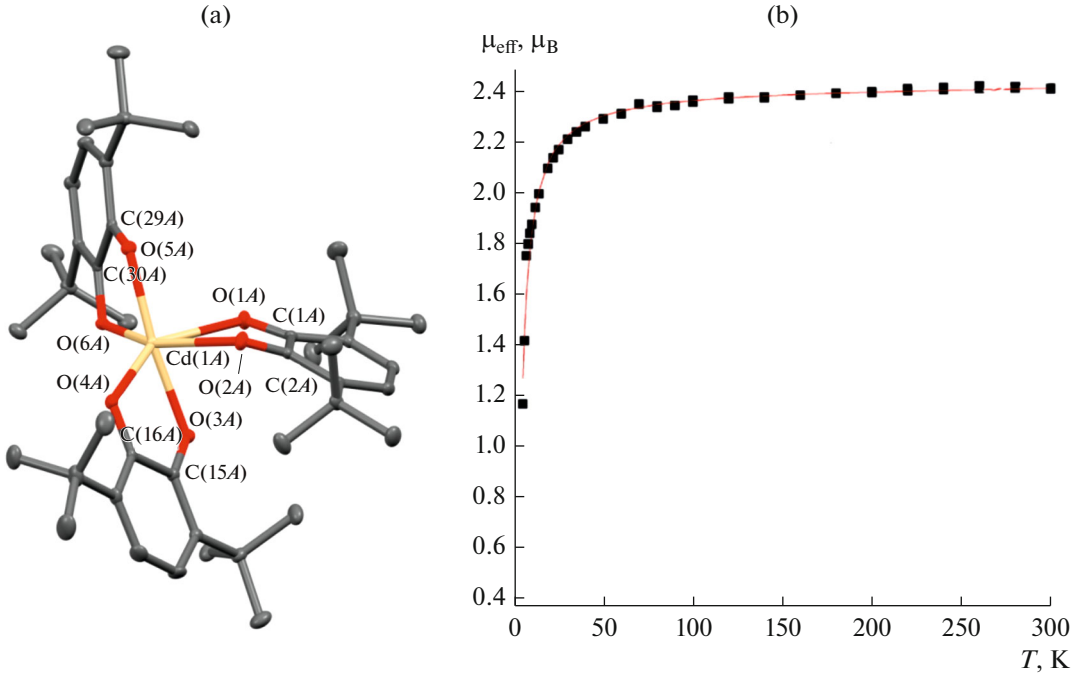

Fig. 2. (a) General view of one of two crystallographically independent molecules of complex **1** and (b) the temperature dependence of the magnetic moment of complex **1**.

magnetic moment equal to 2.41 μ_B (at room temperature) is close to the value (2.45 μ_B) calculated for two noninteracting spins.

The nickel complex (3,6-DBQ)Ni(3,6-DBSQ)$_2$ (**2**) similar in the charge distribution should also be considered [12]. The complex was synthesized by the reaction of nickel carbonyl with an *o*-quinone excess. The bonds lengths distribution in the chelate cycles shows that one of the ligands is coordinated *o*-quinone as in the case of the cadmium complex. The geometry of the internal coordination sphere is close to an octahedron. The twist angle is 41.32°–41.37°. The molecule of complex **2** has the C_2 symmetry axis passing through the nickel atom and coinciding with the local symmetry axis of the ligand. Unlike complex **1**, the neutral *o*-quinone ligand is planar and the radical anions demonstrate a break along the O...O line (13.22°).

The magnetic moment of complex **2** remains almost unchanged with a change in temperature and is equal to 4.57 μ_B (20–300 K), which insignificantly decreases to 4.38 μ_B at the temperatures lower than 20 K. A weak antiferromagnetic interaction of nickel (Ni(II), d^8, $S = 1$) with two semiquinones ($S = 1/2$, $J = -0.2$ cm^{-1}, $g = 2.43$) was observed [12].

Group III of metals in the periodic table is presented in the series of tris(ligand) *o*-dioxolene complexes by seven compounds: two aluminum complexes, three gallium complexes, and two indium complexes. The gallium complexes with three 3,5-di-*tert*-butyl-*o*-benzosemiquinones (Ga(3,5-DBSQ)$_3$

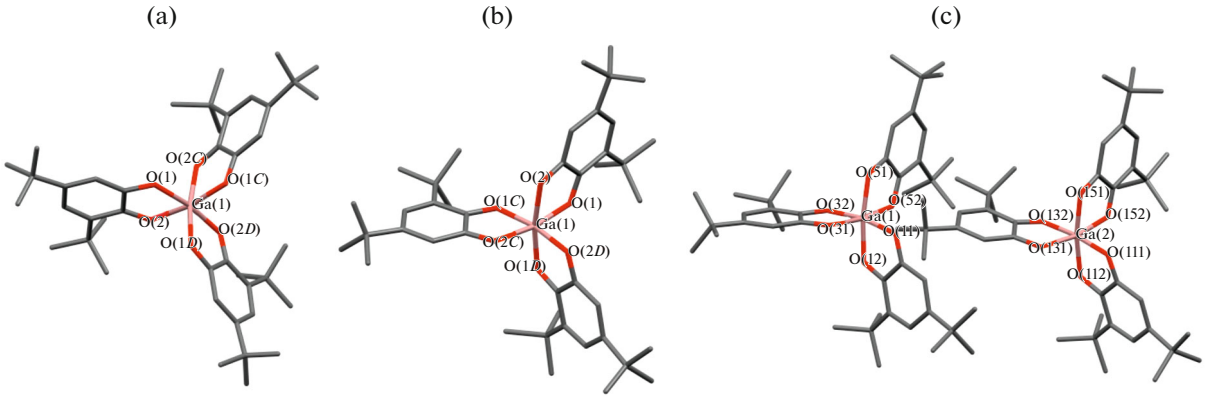

Fig. 3. Gallium complexes with 3,5-di-*tert*-butyl-*o*-benzosemiquinone described in (a) [13], (b) [14], and (c) [15].

(**3**)) were described by three independent research groups [13–15]. It was found in all the three works that the *o*-dioxolene ligands were in the radical-anion form and the geometry of the complexes was a distorted octahedron (Fig. 3). Since 3,5-di-*tert*-butyl-*o*-benzoquinone has no symmetry axis, the tris(ligand) complexes formed by this quinone can be structural and optical isomers. For example, the optical isomer of the complex studied in [13] was described [14].

Although the samples of the complex were synthesized using similar procedures (gallium was dissolved in a toluene solution of *o*-quinone followed by the evaporation of the solvent) the magnetic properties described by independent authors differ. The magnetic moment of the complex was shown [13] to increase monotonically from 2.95 μ_B (320 K) to 3.58 μ_B (9 K) as the temperature decreased, and then magnetic moment decreased to 3.26 μ_B at 2 K. The energy of the ferromagnetic interaction between three unpaired electrons on three semiquinone ligands is 7.8 cm^{-1} ($g = 1.92$). Thus, the ground state of the complex is a quadruplet ($S = 3/2$), which is lower in energy than two degenerated doublet states ($S = 1/2$) by 23.4 cm^{-1}. The ferromagnetic character of the exchange interaction is confirmed by the field dependence of the magnetization at 2–4 K. The authors believe [13] that the predominant ferromagnetic interaction occurs via the vacant 4*p* orbitals of gallium. However, somewhat different magnetic behavior was described in [14]. The value of χT (~0.7 cm^3 K/mol) is weakly temperature dependent and decreases only at the temperatures below 30 K. The high-temperature value is appreciably higher than that for the doublet state and is much lower than χT for the quadruplet state. The triradical ground state in which the quartet state is higher in energy than two degenerated doublet states by 8–20 cm^{-1} was mentioned [14]. The polymorphous modification in which the unit cell contains two symmetrically independent molecules of the same optical isomer as those in [14] was described [15]. The magnetic properties presented in [15] are similar to those described in [13]: χT increases monotonically as the temperature decreases and reaches 1.8 cm^3 K/mol, which is close to the theoretical value for the quadruplet spin state. The energy of the ferromagnetic exchange between the ligand is $J = 17.63$ cm^{-1} ($g = 2.0$). The consideration of the contradiction revealed in the conclusions [13, 15] and [14], especially taking into account the magnetic interactions in the gallium and aluminum complexes with symmetric 3,6-di-*tert*-butyl-*o*-benzosemiquinone described below, allow us to assume a mistake in the results of measurements [14]. Otherwise, the authors worked with different polymorphous modifications of the complex (in the bulk).

The complexes of Group III metals with symmetric 3,6-di-*tert*-butyl-*o*-benzosemiquinone and its derivative, 3,6-di-*tert*-butyl-*o*-benzosemiquinone having the condensed *N*,*N*'-piperazine bicycle in positions 4 and 5, are known. The tris(ligand) aluminum and gallium complexes ($M(3,6\text{-DBSQ})_3$, M = Al (**4**) [16], Ga (**5**)) were synthesized by the exchange reactions of the corresponding halides with thallium *o*-semiquinolate [4]. The complexes are isostructural and, hence, the molecular structure of the gallium compound only is described in detail [4]. The structure of the aluminum complex is studied in detail in the present work. According to the bond lengths, all three ligands exist in the radical-anion form (C–O 1.289–1.294 Å). The structure of the internal coordination sphere is a weakly distorted octahedron (Fig. 4). The twist angle is 44.13°–45.33°. The 2-fold symmetry axis of the molecule passes through the aluminum atom and the middle of one of the ligands. As often observed in similar structures, the planes of the *o*-semiquinone ligands are slightly twisted along the local symmetry axis of the ligand. In addition, there is a slight break along the O...O line of each ligand. However, the total (twist + break) distortions do not exceed 20° (the value of the maximum torsion angle AlO(1)C(1)C(6)).

Ferromagnetic exchange interactions prevail in compounds **4** and **5** as in the above described gallium

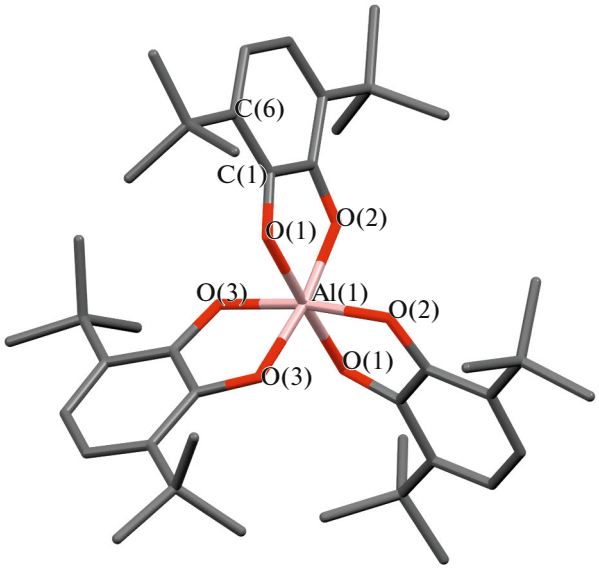

Fig. 4. Molecular structure of the Al(3,6-DBSQ)$_3$ complex.

complexes with 3,5-DBSQ. The magnetic moments of complexes **4** and **5** at room temperature are close to 3.0 μ_B, which corresponds to three noninteracting spins. The temperature decrease leads to a monotonic increase in the effective magnetic moment (μ_{eff}) to 3.62 μ_B (5 K) for the gallium complex and 3.86 μ_B (5 K) for the aluminum compound. The calculation of the exchange interaction energy gave the following values: 6.23 cm^{-1} (g = 1.91) for the gallium complex and 8.55 cm^{-1} (g = 1.93) for the aluminum complex. These values are quite consistent with the results obtained [13] for Ga(3,5-DBSQ)$_3$ (7.8 cm^{-1}, g = 1.92).

Unlike all compounds described above, the indium complex In(3,6-DBSQ)$_3$ (**6**) is characterized by the trigonal prismatic geometry (Fig. 5) [17]. The complex was synthesized by the dissolving of metallic indium in a toluene solution of *o*-quinone. According to the bond lengths in the chelate cycles, the ligands exist in the radical-anion form (C–O 1.270–1.289 Å).

The trigonal prism is slightly distorted. The twist angle is 4.25°–10.21°. The semiquinone ligands are nonplanar. The inflection angles along the O...O line are 4.13°, 7.04°, and 12.99°. Complex **6** is the only representative of the tris-*o*-dioxolene compounds 3,6-DBSQ with the trigonal prismatic coordination environment. This feature is probably related to a larger ionic radius of indium. The ionic radii of the Group III metals are as follows [18]: Al 0.57, Ga 0.62, and In 0.92 Å. Note that the trigonal prismatic geometry of the indium complex is also retained in the anionic form [19]. Reduction occurs through one of the ligands.

Unlike the above described complexes of the Group III metals, the exchange interactions in complex **6** are antiferromagnetic. The value of μ_{eff} at room temperature is close to the value calculated for three noninteracting spins (3.0 μ_B). Cooling decreases μ_{eff} to 0.75 μ_B (4 K) (Fig. 5). This result is associated with the symmetry of the complex. If the vacant *p* orbitals of the metals (Ga, Al) and the π* orbitals of semiquinones in the octahedron are referred to different irreducible representations and, therefore, have the zero overlapping integral, then two of three *p* orbitals of the metal and two of three π* orbitals of semiquinones in the point D_{3h} group are referred to the irreducible representation *E*'. Thus, the nonzero overlapping integral of the magnetic orbitals of the ligands appears and, as a consequence, the channel for the antiferromagnetic interaction is formed.

Four homoligand complexes with the 3,6-di-*tert*-butyl-*o*-benzosemiquinone derivative bearing the *N*,*N*'-piperazine bicycle (3,6-DBSQ-pipe) in positions 4 and 5 were synthesized [20]. All M(3,6-DBSQ-pipe)$_3$ complexes (M = Al (**7**), Ga (**8**), and In (**9**)) were

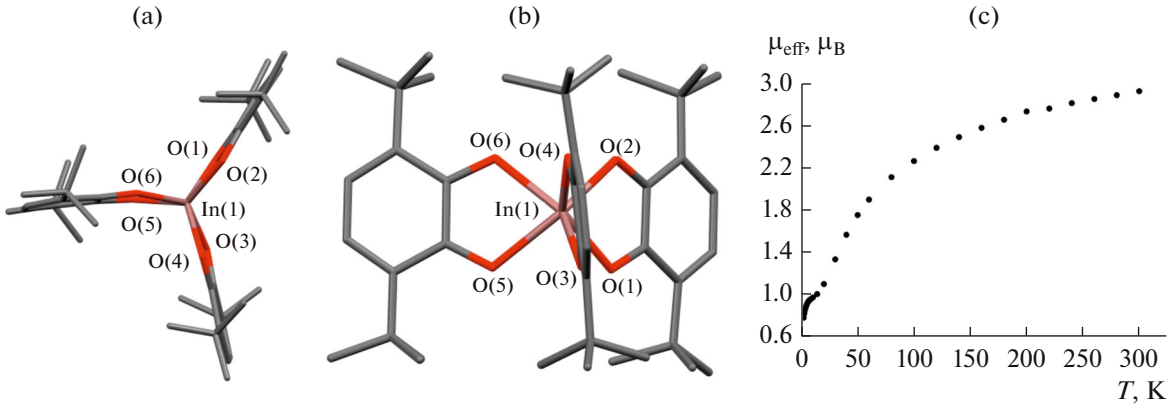

Fig. 5. Molecular structure of the In(3,6-DBSQ)$_3$ complex. The (a) view along the C_3 axis, (b) side view, and (c) temperature dependence of the magnetic moment of the complex.

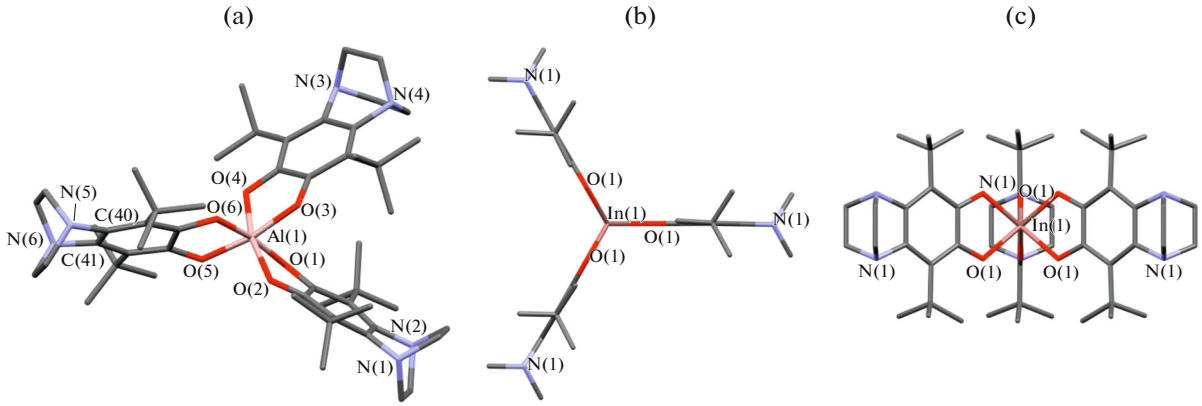

Fig. 6. Structures of the 3,6-DBQ-pipe complexes with (a) aluminum and (b, c) indium (views along the (b) C_3 and (c) C_2 axes).

synthesized by the exchange reactions of metal halides with sodium *o*-semiquinolate. In addition, complex **8** can be prepared by the dissolving of metallic gallium (as an amalgam) in a solution of *o*-quinone. Gallium complex **8** was isolated with two guest THF molecules, and the aluminum complex (**7**) was isolated with one guest molecule of *n*-hexane. The gallium complex similar to complex **8** but without guest solvent molecules was obtained (**8a**). Since the molecular structures of complexes **8** and **8a** differ slightly, only the structure of complex **8** is discussed in this work. The geometry of the aluminum and gallium compounds is a strongly distorted octahedron (Fig. 6). However, this distortion cannot be named prismatic. The twist angles in the complexes are the following: Al (**7**) 38.54°–48.87° and Ga (**8**) 37.98°–42.18°. The OAlO and OGaO angles at the oxygen atoms arranged in the *trans* positions to each other are 166.42°, 169.35°, and 170.02° for the aluminum compound and 164.29°, 168.98°, and 170.51° for the gallium complex, respectively. The bond lengths in the chelate cycles indicate the radical-anion form of the ligands (C–O 1.287–1.295 Å). It should be mentioned that 3,6-DBQ-pipe is one of the most sterically hindered *o*-quinones. This is indicated by the largest torsion angle O=C–C=O in neutral *o*-quinone: 43.7°. The torsion angle considerably increases to 25°–33° when the substituents appear in positions 4 and 5 [21–23]. This angle in 3,6-DBQ is 1.12°. The distinction of 3,6-DBQ-pipe from other *o*-quinones is that the rigid piperazine bicycle competes with the carboxyl group for the space occupied by the methyl groups of the *tert*-butyl substituents. The steric hindrance of *o*-quinone affects the geometry of its radical anion in the complexes. In the complexes with 3,6-DBQ, the methyl groups of the *tert*-butyl substituents always exist in the retarded conformation with respect to the nearest oxygen atom of the carbonyl group in *o*-semiquinone. Both eclipsed and staggered conformations can be met in the complexes with 3,6-DBSQ-pipe. In aluminum complex **7**, two semiquinones have breaks along the O···O line equal to 16.68° and 22.49°, and the third ligand has no break but is twisted along the C_2 local symmetry axis of *o*-semiquinone at an angle of 10.98°. Similar distortions but with distinct angles can be found in the gallium complex (**8**).

As in the case of complex **6**, the indium complex In(3,6-DBSQ-pipe)$_3$ (**9**) [20] differs from the aluminum and gallium complexes. Compound **9** is characterized by an ideal trigonal prismatic geometry (Fig. 6). The molecule of the complex is highly symmetric and belongs to the D_{3h} point group. The bond lengths in the chelate cycles indicate that the ligands exist in the radical-anion form (C–O 1.28 Å). The packing of complex **9** is interesting. The 3-fold axes of all molecules are collinear, and the molecules themselves form layers (Fig. 7).

The magnetic properties of the M(3,6-DBSQ-pipe)$_3$ complexes (M = Al, Ga, In) are similar to those of the above described complexes with 3,6-DBSQ (Fig. 7). Ferromagnetic exchange interactions predominate in the aluminum and gallium compounds, whereas the indium complex is characterized by prevailing antiferromagnetic interactions (J = 18.6 cm^{-1}, zJ' = –2.2 cm^{-1} and J = 10.3 cm^{-1}, zJ' = –0.41 cm^{-1}, g = 2.0 for M = Al and Ga, respectively; J = –28.3 cm^{-1}, zJ' = –6.1 cm^{-1}, g = 2.0 for M = In).

Data on the structurally characterized tris-*o*-dioxolene complexes of the Group IV metals are lacking from the structural database.

Among the Group V metals, the vanadium complex V(3,6-DBCat)$_2$(3,6-DBSQ) (3,6-DBCat is the catecholate dianion 3,6-DBQ) (**10**) was characterized [24]. The geometry of the internal coordination sphere of the complex is close to the octahedral one. The twist angle is 40.42°–41.25°. The OVO angles for the oxygen atom localized in the *trans* positions to each other are 164.25° and 177.81°. According to the bond lengths in the chelate cycle, one of the ligands can be characterized as the radical anion (C–O 1.298 Å). The bond lengths in two other ligands are characteristic of the

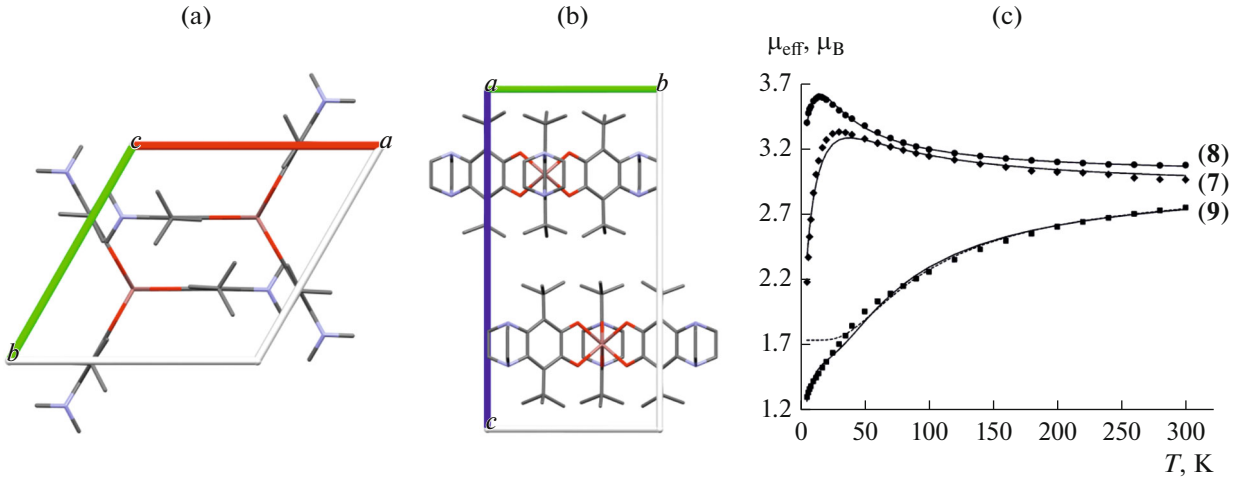

Fig. 7. Packing fragment of the In(3,6-DBSQ-pipe)$_3$ complex (**9**): views along the (a) C_3 and (b) C_2 molecular axes. (c) Temperature dependences of the magnetic moment for the M(3,6-DBSQ-pipe)$_3$ complexes (M = (**7**) Al, (**8**) Ga, and (**9**) In).

dianion–catecholate coordination mode: C–O 1.331 and 1.326 Å. This is consistent with the oxidation state of vanadium +5, d^0. The magnetic properties were not described. The EPR spectrum of a solution of the complex exhibits the hyperfine coupling (HFC) with two protons in positions 4 and 5 (a_{iso}(H) = 4.53 G (2H)) and the HFC on ^{51}V ($I = 7/2$, a_{iso}(V) = 3.47 G) and thus confirms the doublet ligand-centered state. Thus, the single unpaired electron is localized on one semiquinone.

The neutral tris-*o*-dioxolene complexes of the Group VI metals are presented by numerous structures of chromium compounds. The first chromium tris-*o*-semiquinolate Cr(3,5-DBSQ)$_3$ (**11**) was described in 1979 [25], and a similar complex Cr(3,6-DBSQ)$_3$ (**12**) was described in 2007 [26]. Complex **11** was prepared from chromium carbonyl and *o*-quinone, and complex **12** was synthesized by the reaction of metal tetrahydrofuranate trichloride with pyrocatechol in the presence of a base and air oxygen. The geometry of the coordination polyhedron is close to the octahedral for both compounds (Fig. 8). In complex **11**, the OCrO angles for the oxygen atoms occupying the *trans* positions to each other are 170.44°, and those for complex **12** are 169.25° and 177.75°. Interestingly, only one structural and optical isomer, whose molecule is characterized by the ideal C_3 symmetry, was isolated and described for complex **11**. The twist angle is 41.99°. The C–O bond lengths are in the range characteristic of the semiquinone coordination mode (C–O 1.279 and 1.299 Å). The symmetry of the molecule of complex **12** is slightly distorted C_3 (the ideal one is C_2). The twist angle is 42.80°–43.23°. The C–O distances are a little longer than those in complex **11** (1.303–1.310 Å). Thus, the charge distribution in both complexes corresponds to the formula Cr(III)(SQ$^{-\cdot}$)$_3$.

However, in spite of the presence of formally three radical anions, both compounds are diamagnetic. Trivalent chromium (Cr^{3+}, d^3, $S = 3/2$) in the octahedral environment has three unpaired electrons in the t_{2g} block of atomic orbitals. The orbitals of semiquinones on which the unpaired electrons are localized (in the C_{2v} local symmetry of the ligand) in the octahedron have the same symmetry as the t_{2g} orbitals of the metal. This leads to a high overlapping integral of the magnetic orbitals of the ligands and metal and, as a result, to a strong antiferromagnetic interaction and sometimes to diamagnetism. The one-electron reduction of both complexes occurs through the ligand. The EPR spectra for anions **11**$^-$ and **12**$^-$ indicate that the unpaired electron is localized on the metal.

Three new chromium complexes were synthesized by the reaction of (THF)$_3$CrCl$_3$ with sodium *o*-semiquinolate and characterized: Cr(3,6-DBSQ-pipe)$_3$ · C_6H_{14} (**13**), Cr(3,6-DBSQ-pipe)$_3$ · (*iso*-C_5H_{11})$_2$O (**14**), and Cr(3,6-DBSQ-gly)$_3$ (**15**), where 3,6-DBSQ-gly is 3,6-di-*tert*-butyl-*o*-semiquinone with the *O*,*O*'-ethylenedithiolate cyclic substituent in positions 4 and 5 (this work). In complex **13**, the geometry of the internal coordination sphere is close to an octahedron (twist angle 37.13°–39.35°) and all the three ligands differ. The molecular geometry of complex **14** slightly differs from that of complex **13** (twist angle 37.22°–40.84°). The C_2 axis of the molecule of complex **14** passes through the chromium atom and the middle of one of the ligands. The molecule of compound **15**, as well as the molecule of complex **13**, has no symmetry elements: all ligands are different (twist angle 36.24°–38.54°). The C–O bond lengths in complexes **13**–**15** lie in a range of 1.295–1.307 Å, which corresponds to the charge distribution Cr^{3+}(SQ$^{-\cdot}$)$_3$. The temperature dependence of the

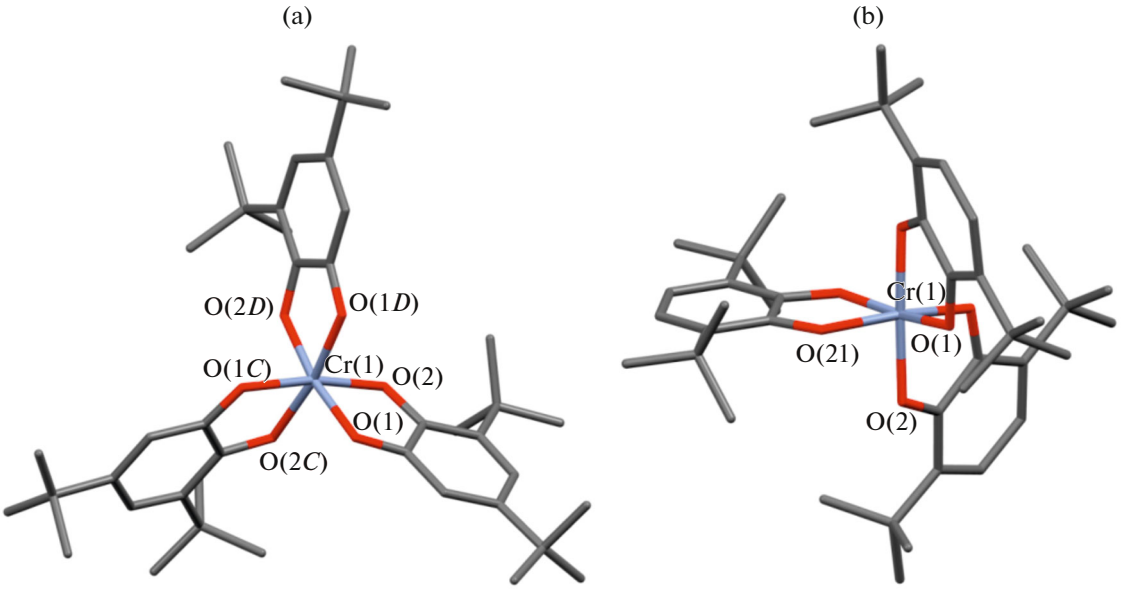

Fig. 8. Molecular structures of the chromium complexes (a) $Cr(3,5\text{-}DBSQ)_3$ and (b) $Cr(3,6\text{-}DBSQ)_3$.

magnetic susceptibility was studied for complexes **13** and **15**.

Unlike two chromium complexes **11** and **12** described above, compounds **13** and **15** are paramagnetic (Fig. 9). The values of μ_{eff} at 2.0 K are 1.30 μ_B for complex **13** and 0.97 μ_B for complex **15**. The high-temperature (300 K) values are the following: 1.69 μ_B for complex **13** and 1.46 μ_B for complex **15**. The $Cr(SQ)_3$ system is even-spin at any charge distribution; i.e., its ground state can be singlet with $S = 0$ and $\mu_{eff} = 0$, triplet with $S = 1$ and $\mu_{eff} = 2.83$, etc. Based on the above considerations, the high-temperature moment of complexes **13** and **15** indicates, most likely, the residual paramagnetism.

Tris(dioxolene) complexes of the Group VII metals are presented by four complexes: two manganese compounds $Mn(3,6\text{-}DBSQ)_2(3,6\text{-}DBCat)$ (**16**) [27] and $Mn(3,6\text{-}DBSQ\text{-}pipe)_2(3,6\text{-}DBCat\text{-}pipe) \cdot 2THF$ (**17**) [28] and the rhenium and technetium complexes $Re(3,5\text{-}DBCat)_3$ (**18**) [29, 30] and $Tc(3,5\text{-}DBCat)_3$ (**19**) [31]. Complexes **16** and **18** were synthesized by the reactions of the corresponding carbonyls with *o*-quinone. Complex **16** was obtained occasionally carrying out the reaction in the presence of 2,2'-dithiophene [27]. Compound **17** was synthesized by the exchange reaction of manganese dichloride with thallium *o*-semiquinolate (2 equiv) in the presence of free *o*-quinone.

$$MnCl_2 + 2\,Tl(3,6\text{-}DBSQ\text{-}pipe) + 3,6\text{-}DBQ\text{-}pipe \xrightarrow{-2\,TlCl} Mn(3,6\text{-}DBSQ\text{-}pipe)_2(3,6\text{-}DBCat\text{-}pipe).$$

The geometry of the internal coordination sphere of manganese complexes **16** and **17** is close to the octahedral (twist angles are 43.93°–45.20° for **16** and 40.64°–44.71° for **17**). The C–O bond lengths in complex **16** are 1.278/1.279, 1.305/1.321, and 1.311/1.311 Å. The first ligand is unambiguously interpreted as the semiquinone radical anion, whereas the C–O bond lengths in two remained ligands are intermediate between those in catecholate and semiquinone. Taking into account the intense charge-transfer Cat–SQ band characteristic of mixed-valence complexes, the charge distribution was interpreted [27] as $Mn(IV)(3,6\text{-}DBCat)(3,6\text{-}DBSQ)_2$ with the delocalized charge between two ligands: $Mn(IV)(SQ)(dioxolene^{-1.5})_2$. A minor decrease in the intensity of this band on heating indicates the beginning of the redox transition

$$Mn(3,6\text{-}DBSQ)_2(3,6\text{-}DBCat) \rightleftharpoons Mn(3,6\text{-}DBSQ)_3.$$

The crystal lattice of complex **17** contains two guest THF molecules. The charge distribution in manganese complex **17** is similar to that in complex **16**. The magnetic moment of complex **16** monotonically and uniformly increases with temperature from 1.67 μ_B at 5 K to 3.71 μ_B at 305 K, whereas μ_{eff} of complex **17** remains nearly unchanged (1.70–1.82 μ_B) in a range of 2–300 K. The ground doublet state of the spin system Mn(IV), d^3; $2(SQ^{-\cdot})$ ($2 \times S = 1/2$) is easily explained

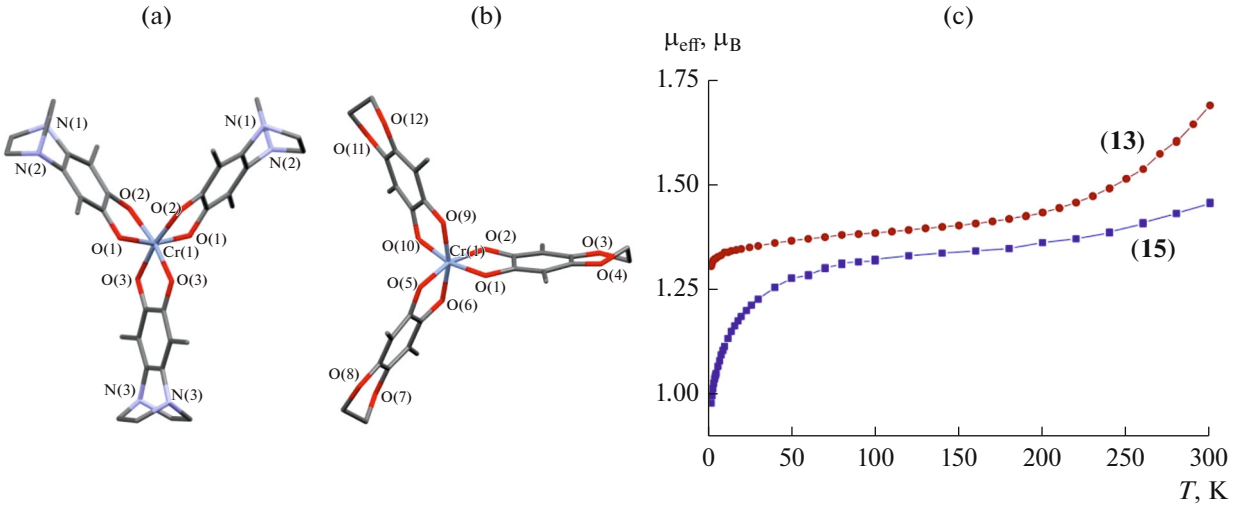

Fig. 9. Molecular geometries of chromium complexes (a) **14** and (b) **15**; (c) the temperature dependences of the magnetic moment for complexes **13** and **15**.

by the strong antiferromagnetic interaction of spins due to the same symmetry of boundary orbitals, as in the case of the chromium complexes; i.e., the unpaired electrons on the π* orbitals of two *o*-semiquinones exhibit a strong antiferromagnetic interaction with unpaired electrons in the t_{2g} block of the atomic orbitals of manganese. The magnetism of the complexes is determined by the spin on manganese. The energies of the magnetic exchange for complex **16** were not presented [27]. Evidently, the magnetism of the complex is determined by the existence of thermally achievable states with a higher multiplicity. At the same time, for complex **17** these states are higher in energy and thermally unachievable.

The original synthetic procedure was described for rhenium complex **18** [32].

$$[ReO_2I(PPh_3)_2] + 3\,H_2(3,5\text{-DBCat}) + 1/2O_2 \xrightarrow{\Delta} [Re(3,5\text{-DBCat})_3] + 2\,PPh_3 + 3\,H_2O + 1/2I_2.$$

The geometry of the internal coordination sphere of the complex is intermediate between an octahedron and a trigonal prism (twist angle 33.08°–37.01°). The C–O bond lengths in the chelate modes of the ligands differ from all above described values: 1.361/1.363, 1.356/1.363, and 1.361/1.372 Å. These values correspond to the catecholate coordination mode of the ligands and, hence, to the charge distribution Re(3,5-DBCat)$_3$. The magnetism of the complex is determined by the single unpaired electron on the metal [29]. The understated magnetic moment (1.18 μ_B at room temperature) is explained [29] by a noticeable contribution of the spin–orbital interaction. The doublet metal-centered state is also confirmed by the EPR spectrum in a solution ($\langle g\rangle = 2.010$ and $a = 0.002$ cm^{-1}, HFC on ^{185}Re and ^{187}Re, $I = 5/2$).

The technetium complex (**19**) similar in composition and charge distribution was synthesized by the reflux of a mixture of salt NH_4TcO_4 with pyrocatechol H_2(3,5-DBCat) in methanol [31]. Its structure resembles the structure of complex **18**. As in the case of the rhenium complex, the magnetism of complex **19** is determined by the single unpaired electron on the metal ($S = 1/2$, $\mu_{eff} = 1.28\ \mu_B$ at room temperature). The EPR spectrum of a solution of the complex exhibits the hyperfine structure (HFS) on ^{99}Tc ($I = 9/2$, $\langle g\rangle = 2.0134$).

Homoligand *o*-dioxolene complexes of the Group VIII metals are presented by four cobalt complexes Co(3,6-DBSQ)$_3$ (**20**) [4], Co(3,6-DBSQ-gly)$_3$ (**21**) [5], Co(3,6-DBSQ-pipe)$_3$ (**22**) [5], and Co(3,6-DBSQ-pipe)$_3$ · C_6H_{14} (**23**) (** this work); two iron complexes Fe(3,5-DBSQ)$_3$ (**24**) [33] and Fe(3,6-DBSQ)$_3$ (**25**) [34]; and ruthenium Ru(3,5-DBSQ)$_3$ (**26**), osmium Os(3,5-DBSQ)$_3$ (**27**) [35, 36], and rhodium Rh(3,5-DBSQ)$_3$ (**28**) [37] compounds. The nickel complex (3,6-DBQ)Ni(3,6-DBSQ)$_2$ (**2**) was discussed above.

Complex Co(3,6-DBSQ)$_3$ (**20**) was synthesized by the reaction of cobalt carbonyl with *o*-quinone. The geometry of the internal coordination sphere is a weakly distorted octahedron (twist angle 47.06°–47.60°). The molecule is symmetric: the C_2 axis passes through the metal atom and halves one of the ligands. The planes of the ligands are slightly distorted. The C–O bond lengths lie in the range characteristic of the coordinated semiquinone radical anion (1.290, 1.295 Å). Thus, the charge distribution in complex **20** is Co(III), d^6, low-spin (surrounded by three radical anions SQ$^{-\cdot}$). According to the data of magnetochemical measurements, the ground spin state of complex

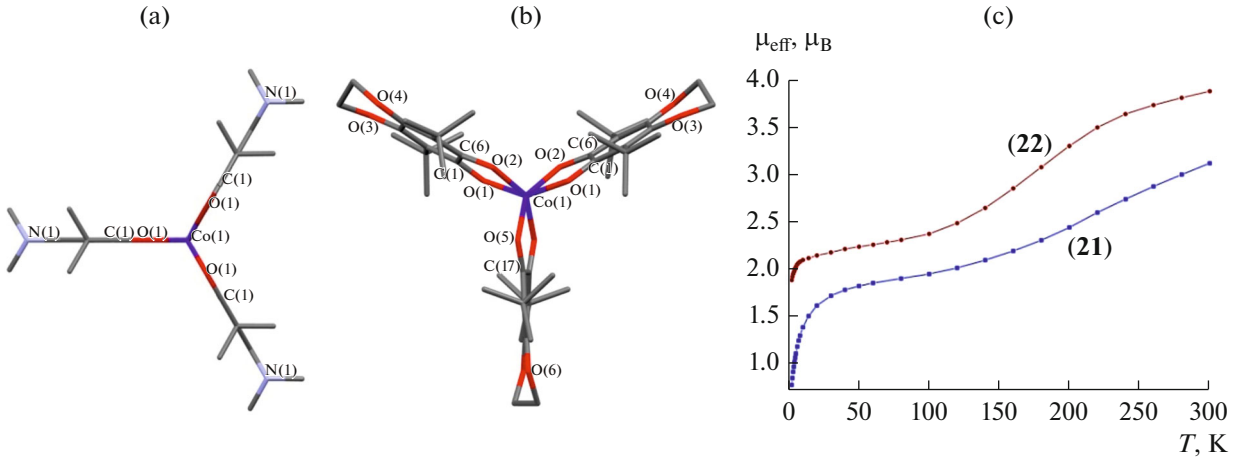

Fig. 10. Molecular structures of complexes (a) **22** and (b) **21** ((b) view along the C_3 axis) and (c) the temperature dependences of the magnetic moment for complexes **22** and **21**.

20 is doublet with $\mu_{eff} = 1.82\ \mu_B$ at 5.0 K. Heating leads to a monotonic increase in the magnetic moment to 3.04 μ_B at 350 K. The high-temperature value equal to 3.04 μ_B is very close to the value calculated for three spins localized on three ligands (3.0 μ_B). In other words, three unpaired electrons of the ligands antiferromagnetically interact via the filled *d* orbitals of the diamagnetic metal. The interaction energy is estimated [4] as $J = -39.1\ cm^{-1}$ ($g = 2.17$). In addition, it is mentioned that in three isostructural complexes Al(3,6-DBSQ)$_3$ (**4**), Ga(3,6-DBSQ)$_3$ (**5**), and Co(3,6-DBSQ)$_3$ (**20**) containing diamagnetic metal atoms the energies of the ligand–ligand magnetic exchange have opposite signs for the transition and nontransition metals: 8.55, 6.23, and $-39.1\ cm^{-1}$ for complexes **4**, **5**, and **20**, respectively [4]. The authors conclude [4] that the participation of the filled *d* orbitals (t_{2g} in O_h (octahedron)) in the group molecular orbitals containing unpaired electrons in complex **20** provides the channel of the antiferromagnetic ligand–ligand interaction.

Three tris(ligand) cobalt complexes containing the cyclic substituents in the *o*-quinone ligands were synthesized later: **21** [5], **22** [5], and **23** (this work). The structure of complex **22** (trigonal prism) is identical to that of the indium compound (**9**) with a similar composition. The molecule is characterized by the symmetry group D_{3h}. The molecular geometry of complex **21** is close to a trigonal prism, and the twist angle is 20.07°–21.21° (Fig. 10). The molecule has the C_2 symmetry axis passing through the metal atom and the local symmetry axis of one of the ligands. According to the conclusions [5], the trigonal prismatic geometry is provided by the C···H and O···H intermolecular interactions. The C–O bond lengths in complex **22** (1.256 Å) have boundary values of the bond lengths characteristic of the semiquinone radical anion. The Co–O bond lengths (1.995 Å) are intermediate between those for Co(II) and Co(III) [38]. In complex **21**, on the contrary, the Co–O bonds are closer to those of high-spin Co(II) (2.020–2.030 Å), whereas the C–O bonds are typically semiquinone ones (1.270–1.273 Å). However, the magnetism of complex **9** is unambiguously interpreted, whereas the magnetic properties of complexes **21** and **22** cannot be interpreted unambiguously. The temperature dependences of the magnetic moment for compounds **21** and **22** are similar with the difference that the values of μ_{eff} for complex **22** are slightly higher than those for complex **21**. The high-temperature values of μ_{eff} (3.11 μ_B for **21** and 3.88 μ_B for **22** at 300 K) exceed the spin-only value (3.0 μ_B) for three noninteracting spins on three ligands bound to the diamagnetic ion Co(III), d^6, low-spin. Thus, it seems impossible to explain the high-temperature value of the magnetic moment only by the presence of radical ligands.

Two models were considered [5] to explain the magnetic properties of complexes **21** and **22**. It was assumed in the framework of the first model that cobalt(III) has the intermediate spin $S = 1$. Together with three unpaired electrons on semiquinones, the calculated value of μ_{eff} of the complex is 4.12 μ_B, which is close to the experimental value at 300 K. A decrease in the magnetic moment with cooling is explained by the antiferromagnetic exchange. The second model assumes the reversible electron transfer (redox isomerism) in the complex to form the high-spin Co(II) surrounded by two semiquinones and one coordinated neutral quinone with the delocalization of two unpaired electrons on three ligands. Both models have arguments pro and contra.

The complex (compound **23**) similar in composition to complex **22** but with a different geometry of the coordination sphere (distorted octahedron) was synthesized using another solvent for crystallization. The presence of hexane as the guest solvent molecule is

enough for the cleavage of the C···H and O···H interactions, which allowed compound **22** to remain in the trigonal prism geometry. The magnetism of the complex was not studied, but the bond lengths indicate that this compound is the typical Co(III) complex with three semiquinones: Co–O 1.862–1.899 Å and C–O 1.283–1.313 Å.

The iron complexes (**24** [33] and **25** [34]) were synthesized by the reaction of iron carbonyl with the corresponding *o*-quinone. The geometry of the internal coordination sphere is intermediate between an octahedron and a trigonal prism: the twist angles for complex **24** are 33.27°–36.95° and those for compound **25** are 37.71°–38.59°. The complexes contain no molecular symmetry axes. The C–O bond lengths indicate that both complexes are the Fe(III) compounds with three semiquinones: C–O 1.275–1.287 Å (**24**) and C–O 1.261–1.288 Å (**25**). According to the magnetochemical data, the ground spin state of complex **24** is triplet ($S = 1$). The magnetic moment is nearly temperature independent, being 2.95 μ_B (285 K), and is interpreted [33] as a result of the interaction of three unpaired electrons of high-spin iron Fe(III), d^5, with three unpaired electrons of semiquinones, since the orbitals of iron (t_{2g} in the distorted octahedron) have the same symmetry as the π^* orbitals of semiquinones. Two electrons that remained on the iron atom determine the magnetism of the complex. The situation for complex **25** is somewhat more complicated. The magnetic moment of complex **25** increases from 2.18 μ_B at 5 K to 4.6 μ_B at 300 K. It is assumed [34] that the ground state of the complex is triplet ($S = 1$). The understated value of μ_{eff} at low temperature is explained by the intermolecular exchange interaction, and an increase in the magnetic moment is explained by the population of the thermally achievable states with a higher multiplicity. However, the magnetic moment does not reach the value (6.63 μ_B) calculated for the system of spins of Fe(III), d^5, $S = 5/2$; 3 × SQ, 3 × $S = 1/2$. The approximation gives the following energies of the antiferromagnetic exchange interaction: $J_{Fe-SQ} = -139$ cm^{-1}, $J_{SQ-SQ} = -235$ cm^{-1}, and $g = 2.12$.

The ruthenium complex (**26**) was synthesized by the exchange reaction of 3,5-di-*tert*-butyl-*o*-semiquinone potassium salt with ruthenium trichloride. Two isomers were structurally characterized: *cis* and *trans* according to the commonly accepted classification [35]. The *cis* isomer has the C_3 symmetry axis, and all *tert*-butyl groups localized in the *ortho* position to the oxygen atom have the same direction. One of the ligands is turned to the opposite direction. The geometry of the internal coordination sphere of both isomers is an octahedron distorted toward a trigonal prism. The twist angles are 49° and 48° in the *trans* and *cis* isomers, respectively. The valent states of the metal and ligands are not unambiguously interpreted [35]. The C–O bond lengths are intermediate between those for semiquinone and catecholate: 1.32 Å and 1.30 Å for the *cis* and *trans* isomers, respectively. An analysis of the Ru–O bonds suggests that the valence of ruthenium is higher than three.

Osmium complex **27** is isostructural to the *trans* isomer of complex **26** [35]. The twist angle is 49°. The averaged C–O bond length is 1.33 Å. All the three complexes (*cis*-**26**, *trans*-**26**, and **27**) are diamagnetic. According to the ^{1}H NMR data, the ruthenium complexes exhibit structural rigidity, whereas the osmium compound is isomerized in a solution to form a racemic mixture of optical isomers [35].

Tris(ligand) complex **28** was synthesized by the reaction of rhodium trichoride with pyrocatechol [37]. Two symmetrically independent molecules in the unit cell are optical isomers. The coordination polyhedron is a distorted octahedron. The twist angles are 43.65°–46.87° for one molecule and 42.22°–48.12° for another molecule. It should be mentioned that an averaged value of 1.31 Å is characteristic of coordinated semiquinone in spite of the very high scatter in C–O bond lengths (1.26–1.37 Å in one molecule and 1.28–1.34 Å in another molecule). The ground state of the complex is doublet, which is indicated by the EPR spectrum with $g_i = 2.00$. Compound **28** and similar in composition cobalt complex **20** demonstrate similar magnetic behavior, but the states with a higher multiplicity are thermally unachievable in the rhodium compound. Thus, diamagnetic Rh(III) (d^6) is coordinated by three semiquinones, two of which are bound by a strong antiferromagnetic interaction.

Several conclusions can be made after the analysis of the complexes listed above (Table 1).

(1) In molecules of the tris(dioxolene) complexes with the axial symmetry, the ligand situated on the axis is always slightly twisted relative to this axis. Two other ligands have breaks along the O...O line. The same observation concerns the most part of other complexes, but the break along the O...O line can be accompanied with twisting.

(2) The most part of the complexes is characterized by a distorted octahedral geometry of the internal coordination sphere. The twist angle is 40° ± 5° in many complexes. Other complexes are characterized by the geometry close to a trigonal prism.

(3) The complexes with the geometry of a trigonal prism (**9** and **22**) have a pronounced layered (2D) packing in which the molecular axes (or pseudo-axes (**21**)) of 3-fold symmetry are collinear. The exception is complex **6**.

(4) The indium complex with the trigonal prismatic geometry (**6**) was described in 2011 [17]. The data on two cobalt complexes (**22** and **21**) were published later (in 2012), one of which had the ideal geometry and the geometry of another complex was a weakly distorted prism [5]. Complex **23** of the same composition as complex **22** but with the distorted octahedral geome-

Table 1. Symmetry groups, cell parameters, literature sources, and experimental temperatures for complexes **1**–**26**

Metal	Complex	Symmetry group	Cell parameters (Å, deg)	Literature	Conditions*
Cd	$Cd(3,6\text{-}DBSQ)_2(3,6\text{-}DBQ)$ (**1**)	$P\bar{1}$	$a = 14.5473(16)$, $b = 17.5614(19)$, $c = 17.6309(19)$ Å, $\alpha = 93.821(2)°$, $\beta = 101.263(2)°$, $\gamma = 109.323(2)°$, $Z = 4$	10	100 K
Al	$Al(3,6\text{-}DBSQ)_3$ (**4**)	$C2/c$	$a = 21.8759(13)$, $b = 19.1976(9)$, $c = 10.1066(5)$ Å, $\alpha = 90°$, $\beta = 95.189(4)°$, $\gamma = 90°$, $Z = 4$	4	RT
	$Al(3,6\text{-}DBSQ\text{-}pipe)_3 \cdot C_6H_{14}$ (**7**)	Cc	$a = 11.0539(17)$, $b = 26.734(4)$, $c = 19.629(3)$ Å, $\alpha = 90°$, $\beta = 95.180(4)°$, $\gamma = 90°$, $Z = 4$	20	RT
Ga	$Ga(3,5\text{-}DBSQ)_3$ (**3**)	$R3$	$a = 16.419(2)$, $b = 16.419(2)$, $c = 13.899(3)$ Å, $\alpha = 90°$, $\beta = 90°$, $\gamma = 120°$, $Z = 3$	13	RT
	$Ga(3,5\text{-}DBSQ)_3$ (**3**)	$R3$	$a = 16.408(6)$, $b = 16.408(6)$, $c = 13.898(4)$ Å, $\alpha = 90°$, $\beta = 90°$, $\gamma = 120°$, $Z = 3$	14	RT
	$Ga(3,5\text{-}DBSQ)_3$ (**3**)	$P\bar{1}$	$a = 12.7500(16)$, $b = 13.1264(16)$, $c = 13.4477(16)$ Å, $\alpha = 76.352(5)°$, $\beta = 77.706(5)°$, $\gamma = 74.690(5)°$, $Z = 2$	15	100 K
	$Ga(3,6\text{-}DBSQ)_3$ (**5**)	$C2/c$	$a = 22.069(6)$, $b = 19.365(5)$, $c = 10.163(3)$ Å, $\alpha = 90°$, $\beta = 94.90(2)°$, $\gamma = 90°$, $Z = 4$	4	RT
	$Ga(3,6\text{-}DBSQ\text{-}pipe)_3 \cdot 2THF$ (**8a**)	$Pca2_1$	$a = 26.7864(11)$, $b = 11.1805(5)$, $c = 19.6718(8)$ Å, $\alpha = 90°$, $\beta = 90°$, $\gamma = 90°$, $Z = 4$	20	100 K
	$Ga(3,6\text{-}DBSQ\text{-}pipe)_3$ (**8**)	$P2_1/n$	$a = 13.9391(7)$, $b = 24.4087(12)$, $c = 15.0333(7)$ Å, $\alpha = 90°$, $\beta = 92.844(1)°$, $\gamma = 90°$, $Z = 4$	**	100 K
In	$In(3,6\text{-}DBSQ)_3$ (**6**)	$P2_1/n$	$a = 11.3435(4)$, $b = 10.0725(4)$, $c = 36.4349(14)$ Å, $\alpha = 90°$, $\beta = 90.265(1)°$, $\gamma = 90°$, $Z = 4$	4	100 K
	$In(3,6\text{-}DBSQ\text{-}pipe)_3$ (**9**)	$P6_3/m$	$a = 12.0295(4)$, $b = 12.0295(4)$, $c = 20.5222(11)$ Å, $\alpha = 90°$, $\beta = 90°$, $\gamma = 120°$, $Z = 2$	20	100 K
V	$V(3,6\text{-}DBCat)_2(3,6\text{-}DBSQ)$ (**10**)	$Ccca$	$a = 19.9969(17)$, $b = 23.740(2)$, $c = 18.1741(16)$ Å, $\alpha = 90°$, $\beta = 90°$, $\gamma = 90°$, $Z = 8$	22	RT

Table 1. (Contd.)

Metal	Complex	Symmetry group	Cell parameters (Å, deg)	Literature	Conditions*
Cr	$Cr(3,5\text{-}DBSQ)_3$ (**11**)	*R*3	$a = 16.385(3)$, $b = 16.385(3)$, $c = 13.874(4)$ Å, $\alpha = 90°$, $\beta = 90°$, $\gamma = 120°$, $Z = 3$	23	RT
	$Cr(3,6\text{-}DBSQ)_3$ (**12**)	*C*2/*c*	$a = 22.1182(9)$, $b = 19.1114(9)$, $c = 10.0921(3)$ Å, $\alpha = 90°$, $\beta = 95.184(5)°$, $\gamma = 90°$, $Z = 4$	24	100 K
	$Cr(3,6\text{-}DBSQ\text{-}pipe)_3 \cdot C_6H_{14}$ (**13**)	$P2_1/c$	$a = 15.0706(11)$, $b = 26.400(2)$, $c = 14.2269(11)$ Å, $\alpha = 90°$, $\beta = 91.525(2)°$, $\gamma = 90°$, $Z = 3$	**	100 K
	$Cr(3,6\text{-}DBSQ\text{-}pipe)_3 \cdot$ *iso*-$(C_5H_{11})_2O$ (**14**)	*C*2/*c*	$a = 15.0692(13)$, $b = 23.844(2)$, $c = 19.0140(16)$ Å, $\alpha = 90°$, $\beta = 112.880(2)°$, $\gamma = 90°$, $Z = 4$	**	100 K
	$Cr(3,6\text{-}DBSQ\text{-}gly)_3$ (**15**)	$P2_1/c$	$a = 21.0214(8)$, $b = 19.7460(7)$, $c = 11.8423(4)$ Å, $\alpha = 90°$, $\beta = 103.577(1)$, $\gamma = 90°$, $Z = 3$	**	100 K
Mn	Mn(3,6-DBCat) $(3,6\text{-}DBSQ)_2$ (**16**)	$P\bar{1}$	$a = 10.3000(10)$, $b = 10.9510(10)$, $c = 19.298(3)$ Å, $\alpha = 88.970(10)°$, $\beta = 79.600(10)°$, $\gamma = 82.270(10)°$, $Z = 2$	25	RT
	Mn(3,6-DBCat-pipe)$(3,6\text{-}DBSQ\text{-}pipe)_2 \cdot$ 2THF (**17**)	$Pca2_1$	$a = 26.6369(18)$, $b = 11.0435(7)$, $c = 19.5293(13)$ Å, $\alpha = 90°$, $\beta = 90°$, $\gamma = 90°$, $Z = 4$	**	100 K
Re	$Re(3,5\text{-}DBCat)_3$ (**18**)	$P2_1/n$	$a = 15.8455(3)$, $b = 15.8343(3)$, $c = 16.3301(3)$ Å, $\alpha = 90°$, $\beta = 93.3339(9)°$, $\gamma = 90°$, $Z = 4$	27	200 K
Tc	$Tc(3,5\text{-}DBCat)_3$ (**19**)	$P2_1/n$	$a = 15.892(3)$, $b = 15.878(4)$, $c = 16.367(3)$ Å, $\alpha = 90°$, $\beta = 93.13(1)°$, $\gamma = 90°$, $Z = 4$	28	RT
Co	$Co(3,6\text{-}DBSQ)_3$ (**20**)	*C*2/*c*	$a = 21.799(9)$, $b = 19.376(8)$, $c = 10.167(3)$ Å, $\alpha = 90°$, $\beta = 94.99(3)°$, $\gamma = 90°$, $Z = 4$	4	RT
	$Co(3,6\text{-}DBSQ\text{-}gly)_3$ (**21**)	*Pbcn*	$a = 20.0108(12)$, $b = 11.4870(8)$, $c = 20.8327(13)$ Å, $\alpha = 90°$, $\beta = 90°$, $\gamma = 90°$, $Z = 4$	5	150 K
	$Co(3,6\text{-}DBSQ\text{-}pipe)_3$ (**22**)	$P6_3/m$	$a = 11.9045(3)$, $b = 11.9045(3)$, $c = 20.6413(9)$ Å, $\alpha = 90°$, $\beta = 90°$, $\gamma = 120°$, $Z = 2$	5	100 K
	$Co(3,6\text{-}DBSQ\text{-}pipe)_3 \cdot C_6H_{14}$ (**23**)	*Pbca*	$a = 19.5724(18)$, $b = 21.9542(19)$, $c = 26.825(3)$ Å, $\alpha = 90°$, $\beta = 90°$, $\gamma = 90°$, $Z = 8$	**	100 K

Table 1. (Contd.)

Metal	Complex	Symmetry group	Cell parameters (Å, deg)	Literature	Conditions*
Fe	$Fe(3,5\text{-}DBSQ)_3$ (**24**)	$P2_1/n$	$a = 15.904(3)$, $b = 15.891(3)$, c 16.450(4) Å, $\alpha = 90°$, $\beta = 93.22(2)°$, $\gamma = 90°$, $Z = 4$	30	RT
	$Fe(3,6\text{-}DBSQ)_3$ (**25**)	*Pbca*	$a = 18.277(5)$, $b = 11.634(3)$, $c = 39.903(10)$ Å, $\alpha = 90°$, $\beta = 90°$, $\gamma = 90°$, $Z = 8$	31	RT
Ni	$Ni(3,6\text{-}DBSQ)_2(3,6\text{-}DBQ) \cdot C_6H_{12}$ (**2**)	*Ccca*	$a = 20.092(6)$, $b = 24.335(8)$, $c = 18.340(4)$ Å, $\alpha = 90°$, $\beta = 90°$, $\gamma = 90°$, $Z = 8$	12	RT
Ru	Ru(3,5-DBQ)-*cis* (**26**)	*P*	$a = 10.210(3)$, $b = 11.812(4)$, $c = 19.052(6)$ Å, $\alpha = 77.78(3)°$, $\beta = 81.23°$, $\gamma = 85.05°$, $Z = 2$	32	198 K
	Ru(3,5-DBQ)-*trans*	$P2_1/c$	$a = 19.357(9)$, $b = 10.579(6)$, $c = 20.669(11)$ Å, $\alpha = 90°$, $\beta = 97.73(4)°$, $\gamma = 90°$, $Z = 4$	32	RT
Os	$Os(3,5\text{-}DBQ)_3$ (**27**)	$P2_1/c$	$a = 19.278(7)$, $b = 10.487(6)$, c 20.689(9) Å, $\alpha = 90°$, $\beta = 98.11(3)°$, $\gamma = 90°$, $Z = 4$	32	213 K
Rh	$Rh(3,5\text{-}DBSQ)_3$ (**28**)	*Cc*	$a = 11.2499(16)$, $b = 33.145(5)$, $c = 24.000(3)$ Å, $\alpha = 90°$, $\beta = 102.819(10)°$, $\gamma = 90°$, $Z = 8$	34	RT

* RT is room temperature.
** This work.

try containing the guest *n*-hexane molecule was occasionally obtained a little later (this work). It was assumed that the presence or absence of solvent guest molecules in the crystal lattice of the compound prevented the formation of intermolecular interactions and, correspondingly, determined the geometry of the complex. To confirm this proposition, a series of the Group III compounds was obtained (complexes **7**, **8**, **8a**, and **9** [20]), as well as chromium complexes **13**, **14**, and **22** (this work). Some of them were specially crystallized from various solvents, including those whose molecules are too large for incorporation into the lattice of the complex (e.g., complex **8**). However, the assumption was not confirmed. The geometry of the internal coordination sphere is determined by the ionic radius (as in the case of indium, 0.92 Å) or intermolecular contacts (as in the case of cobalt).

The magnetic properties of the complexes represent a regular consequence of peculiarities of the geometry of their coordination polyhedra and charge distribution. For example, the magnetism in the cadmium complex (**1**) is determined by two spins on the ligands that weakly interact with each other, unlike complexes **4** and **5**, where the interaction between the ligands is ferromagnetic. A probable reason is the symmetry. In the cadmium complex, the ligands are strongly distorted and the coordination polyhedron is far from octahedron. As a consequence of the low symmetry, the magnetic orbitals of the ligands are characterized by nonzero overlapping integrals. At the same time, the coordination environment of the metal in the aluminum and gallium complexes is close to octahedra. The orbitals have no possibilities for overlapping, and the unpaired electrons localized on them interact ferromagnetically. Indium compounds **6** and **9** with the coordination geometry of a trigonal prism demonstrate the antiferromagnetic interaction of the ligands, because in the trigonal prism two of three ligands and two orbitals of the metal belong to one irreducible representation, which results in their effective mixing. The chromium (**12**) and iron (**25**) complexes exhibit the strong metal–ligand antiferromag-

Table 2. Crystallographic data and structure refinement details for complexes **4**, **13**–**15**, and **23**

Parameter	Value				
	4	**13**	**14**	**15**	**23**
Formula	$C_{42}H_{60}AlO_6$	$C_{61}H_{86}CrN_6O_6$	$C_{59}H_{89}CrN_6O_{6.5}$	$C_{48}H_{66}CrO_{12}$	$C_{60}H_{92}CoN_6O_6$
FW	687.88	1051.36	1038.36	887.01	1052.32
Temperature, K	100(2)	100(2)	100(2)	100(2)	100(2)
Wavelength, Å	0.71073	0.71073	0.71073	0.71073	0.71073
Crystal system	Monoclinic	Monoclinic	Monoclinic	Monoclinic	Orthorhombic
Space group	*C*2/*c*	$P2_1/c$	*C*2/*c*	$P2_1/c$	*Pbca*
Cell parameters:					
a, Å	21.8759(12)	15.0706(11)	15.0692(13)	21.0214(8)	19.5724(18)
b, Å	19.1976(9)	26.400(2)	23.844(2)	19.7460(7)	21.9542(19)
c, Å	10.1066(5)	14.2269(11)	19.0140(16)	11.8423(4)	26.825(3)
β, deg	95.189(4)	91.525(2)	112.880(2)	103.577(1)	
Volume, $Å^3$	4227.0(4)	5658.3(7)	6294.5(9)	4778.2(3)	11526.6(18)
Z; ρ, g/cm^3	4; 1.081	4; 1.234	4; 1.096	4; 1.233	8; 1.213
μ, mm^{-1}	0.089	0.258	0.231	0.298	0.352
θ, deg	3.32–26.00	2.09–25.00	2.33–25.00	1.99–26.00	1.86–30.05
Number of measured/ independent reflections	13762/4150	44536/9918	24526/5468	40706/9357	84460/16140
R_{int}	0.0466	0.0945	0.0724	0.0398	0.0934
GOOF	1.033	0.947	1.004	1.032	1.115
R_1, wR_2 ($I > 2\sigma(I)$)	0.0486, 0.1121	0.0537, 0.1118	0.0899, 0.2331	0.0463, 0.1143	0.1080, 0.2476
R_1, wR_2 (all reflections)	0.0748, 0.1221	0.1113, 0.1279	0.1330, 0.2626	0.0656, 0.1225	0.1635, 0.2798
Residual electron density ($\Delta\rho_{max}/\Delta\rho_{min}$), e $Å^3$	0.388/–0.216	0.752/–0.447	1.213/–0.506	1.252/–0.397	1.080/–0.957

netic interaction. The reason is the same: three unpaired electrons in the t_{2g} block of the atomic orbitals in the octahedron efficiently interact with unpaired electrons of the ligands of the same symmetry. However, ambiguous interpretations of the magnetic properties are also met, for example, for cobalt complexes **21** and **22**. As already mentioned, their magnetic properties were interpreted in the framework of two models each of which can be considered.

EXPERIMENTAL

X-ray diffraction data were collected on SMART APEX (for **13**, **14**, **15**, and **23**) and Agilent Xcalibur E (for **4**) automated diffractometers (ω and φ scan modes, MoK_α radiation, λ = 0.71073 Å). Experimental sets of intensities were integrated using the SAINT Plus [39] and CrysAlisPro [40] programs for complexes **13**–**15**, **23**, and **4**, respectively. All structures were solved by a direct method and refined by full-matrix least squares for F^2_{hkl} using the SHELXTL program package [41] in the anisotropic approximation for non-hydrogen atoms. Hydrogen atoms were placed in the geometrically calculated positions and refined isotropically. Absorption corrections were applied using the SADABS [42] (for **13**–**15** and **23**) and SCALE3 ABSPACK (for **4**) [43] programs. The crystals of complexes **23** and **13** contain solvate molecules of *n*-hexane and toluene, respectively, disordered over two common positions. In the crystals of complex **23**, the whole molecule of the cobalt complex is disordered over two positions with populations of ~0.87 and 0.13. One of the *t*-Bu groups in complex **14** was found to be disordered over two positions. The solvate molecule of di-*iso*-amyl ether was also found in the crystal of complex **14** in the partial position (on the rotation C_2 axis). The ratio of molecules of the ether and chromium complex in compound **14** is 1 : 2. The main crystallographic data and experimental X-ray diffraction parameters are presented in Table 2.

The structures were deposited with the Cambridge Crystallographic Data Centre (CIF files CCDC nos. 1956614 (**23**), 1956615 (**4**), 1956616 (**15**), 1956617 (**13**), and 1956618 (**14**); ccdc.cam.ac.uk/getstructures).

Synthesis of complex 23. A solution of 2,2'-(pyridine-2,6-diyl)bis(N^1,N^1,N^3,N^3-tetramethylpropane-1,3-diamine (0.024 g, 0.08 mmol) in *n*-heptane (~15 mL) was poured to a solution of tris(4,5-*N*,*N*'-piperazino-3,6-di-*tert*-butyl-*o*-semiquinolate)cobalt(III) (0.155 g, 0.16 mmol) in diethyl ether (~20 mL). The resulting solution was concentrated to a volume of 15 mL. After evaporation, the solution was kept at room temperature for 24 h. The precipitated dark green finely crystalline powder was filtered off, washed with cold heptane, and dried in vacuo. The yield was low: several crystals.

Synthesis of complexes 13–15. A solution of the corresponding *o*-quinone (0.5 mmol) in THF (15 mL) was poured to metallic sodium (2.3 g, 0.1 mol), and the mixture was stirred until the initial color of quinone disappeared completely and a pale yellow solution of sodium catecholate was formed. The obtained solution was separated from a metal excess and poured to a solution of the same *o*-quinone (0.5 mmol) in THF (10 mL). The resulting blue-violet solution was poured to a solution of chromium(III) bis(tetrahydrofuranate trichloride) $CrCl_3 \cdot 2THF$ (0.33 mmol) in THF (5 mL) with permanent stirring. The reaction mixture instantly gained the crimson color. The THF solvent was replaced by hexane, and the solution was filtered. The filtrate was concentrated to 20% of the initial volume and kept at −18°C for 24 h, resulting in the formation of finely crystalline complexes. The yields were 0.3 g (86%) and 0.25 g (84.5%) for complexes **13** and **15**, respectively. Complex **14** was obtained by the recrystallization of compound **13** from di-*iso*-amyl ether.

For $C_{48}H_{66}O_{12}Cr$ (**15**)

Anal. calcd., %	C, 64.99	H, 7.50
Found, %	C, 65.27	H, 7.64

IR (ν, cm^{-1}): 1518 s, 1483 m, 1415 s, 1400 s, 1360 m, 1340 s, 1317 s, 1228 w, 1216 m, 1174 m, 1111 s, 1067 w, 1031 w, 989 s, 963 s, 930 w, 891 s, 877 w, 795 w, 784 m, 707 w, 665 m.

For $C_{60}H_{92}N_6O_6Cr$ (**13**)

Anal. calcd., %	C, 68.93	H, 8.87
Found, %	C, 68.80	H, 8.75

IR (ν, cm^{-1}): 1515 m, 1480 m, 1430 m, 1402 s, 1392 m, 1365 m, 1360 m, 1350 m, 1340 m, 1314 m, 1294 w, 1224 m, 1217 m, 1212 m, 1196 w, 1180 m, 1122 m, 1075 w, 1057 s, 1050 s, 1000 s, 983 s, 935 w, 898 w, 867 w, 853 s, 815 m, 796 w, 773 s, 682 w.

ACKNOWLEDGMENTS

This work was carried out using the scientific equipment of the Center for Collective Use "Analytical Center of the Razuvaev Institute of Organometallic Chemistry of the Russian Academy of Sciences."

FUNDING

This work was carried out in the framework of the state task, theme no. 44.1.

CONFLICT OF INTEREST

The authors declare that they have no conflicts of interest.

REFERENCES

1. Pierpont, C.G. *Coord. Chem. Rev.*, 2001, vols. 219–221, p. 415.
2. Pierpont, C.G. and Kelly, J.K., *PATAI'S Chemistry of Functional Groups*, John Wiley, 2013, p. 1.
3. Buchanan, R.M. and Pierpont, C.G., *Inorg. Chem.*, 1979, vol. 18, p. 3439.
4. Lange, C.W., Conklin, B.J., and Pierpont, C.G., *Inorg. Chem.*, 1994, vol. 33, p. 1276.
5. Bubnov, M.P., Skorodumova, N.A., Baranov, E.V., et al., *Inorg. Chim. Acta*, 2012, vol. 392, p. 84.
6. Sofen, S.R., Ware, D.C., and Cooper, S.R., *Inorg. Chem.*, 1979, vol. 18, p. 234.
7. Pierpont, C.G. and Buchanan, R.M., *Coord. Chem. Rev.*, 1981, vol. 38, p. 45.
8. Brown, S.N., *Inorg. Chem.*, 2012, vol. 51, p. 1251.
9. Piskunov, A.V., Lado, A.V., Abakumov, G.A., et al., *Izv. Akad. Nauk, Ser. Khim.*, 2007, no. 1, p. 92.
10. Bellan, E.V., Poddel'sky, A.I., Protasenko, N.A. et al., *Inorg. Chem. Commun.*, 2014, vol. 50, p. 1.
11. Stiefel, E.I. and Brown, G.F., *Inorg. Chem.*, 1972, vol. 11, p. 434.
12. Lange, C.W. and Pierpont, C.G., *Inorg Chim. Acta*, 1997, vol. 263, p. 219.
13. Adams, D.M., Rheingold, A.L., Dei, A., et al., *Angew. Chem., Int. Ed. Engl.*, 1993, vol. 32, p. 391.
14. Ozarowski, A., McGarvey, B.R., El-Hadad, A., et al., *Inorg. Chem.*, 1993, vol. 32, p. 841.
15. Das, C., Shukla, P., Sorace, L., et al., *Dalton Trans.*, 2017, vol. 46, p. 1439.
16. Piskunov, A.V., Maleeva, A.V., Fukin, G.K., et al., *Russ. J. Coord. Chem.*, 2010, vol. 36, no. 3, p. 161. https://doi.org/10.1134/S1070328410030012
17. Piskunov, A.V., Maleeva, A.V., Fukin, G.K., et al., *Dalton Trans.*, 2011, vol. 40, p. 718.
18. Bokii, G.B. *Vvedenie v kristallokhimiyu* (Introduction to Crystal Chemistry), Moscow: MGU, 1954.
19. Ilyakina, E.V., Poddel'sky, A.I., Piskunov, A.V., et al., *New J. Chem.*, 2012, vol. 36, p. 1944.
20. Piskunov, A.V., Meshcheryakova, I.N., Maleeva, A.V., et al., *Eur. J. Inorg. Chem.*, 2014, p. 3252.

21. Kuropatov, V., Klementieva, S., Fukin, G., et al., *Tetrahedron*, 2010, vol. 66, p. 7605.
22. Shurygina, M.P., Druzhkov, N.O., Arsen'ev, M.V., et al., *Russ. J. Org. Chem.*, 2011, vol. 47, p. 490.
23. Fukin, G.K., Cherkasov, A.V., Shurygina, M.P., et al., *Struct. Chem.*, 2010, vol. 21, p. 607.
24. Morris, A.M., Pierpont, C.G., and Finke, R.G., *Inorg. Chem.*, 2009, vol. 48, p. 3496.
25. Sofen, S.R., Ware, D.C., Cooper, S.R., et al., *Inorg. Chem.*, 1979, vol. 18, p. 234.
26. Kapre, R.R., Bothe, E., Weyhermuller, T., et al., *Inorg. Chem.*, 2007, vol. 46, p. 7827.
27. Attia, A.S. and Pierpont, C.G., *Inorg. Chem.*, 1998, vol. 37, p. 3051.
28. Bubnov, M., Teplova, I., Kozhanov, K., et al., *Inorg. Chim. Acta*, 2019, vol. 486, p. 113.
29. DeLearie, L.A. and Pierpont, C.G., *J. Am. Chem. Soc.*, 1986, vol. 108, p. 6393.
30. Delearie, L.A., Haltiwanger, R.C., and Pierpont, C.G., *Inorg. Chem.*, 1987, vol. 26, p. 817.
31. Delearie, L.A., Haltiwanger, R.C., and Pierpont, C.G., *J. Am. Chem. Soc.*, 1989, vol. 111, p. 4324.
32. Gerber, T.I.A., Luzipo, D., and Mayer, P., *J. Coord. Chem.*, 2004, vol. 57, no. 10, p. 893.
33. Boone, S.R., Purser, G.H., Chang, H.R., et al., *J. Am. Chem. Soc.*, 1989, vol. 111, p. 2292.
34. Attia, A.S., Conklin, B.J., Lange, C.W., et al., *Inorg. Chem.*, 1996, vol. 35, p. 1033.
35. Bhattacharya, S., Boone, S.R., Fox, G.A., et al., *J. Am. Chem. Soc.*, 1990, vol. 112, p. 1088.
36. Hursthouse, M.B., Fram, T., and New, L., *Transition Met. Chem.*, 1978, vol. 3, p. 255.
37. Sengupta, P. and Bhattacharya, S., *J. Indian Chem. Soc.*, 2013, vol. 90, no. 2, p. 169.
38. Adams, D.M., Dei, A., Rheingold, A.L., et al., *J. Am. Chem. Soc.*, 1993, vol. 115, p. 8221.
39. *SAINT Plus. Data Reduction and Correction Program. Version 6.45a*, Madison: Bruker AXS, 2003.
40. *Data Collection, Reduction and Correction Program. CrysAlisPro Software Package*, Agilent Technologies, 2012.
41. Sheldrick, G.M., *SHELXTL. Version 6.14. Structure Determination Software Suite*, Madison: Bruker AXS, 2003.
42. Sheldrick G.M., *SADABS. Version 2.01. Bruker Siemens Area Detector Absorption Correction Program*, Madison: Bruker AXS, 1998.
43. *SCALE3 ABSPACK: Empirical Absorption Correction. CrysAlisPro Software Package*, Agilent Technologies, 2012.

Translated by E. Yablonskaya